

Influence of an inner disc on the orbital evolution of massive planets migrating in resonance

Aurélien Crida¹, Zsolt Sándor^{2,3} and Willy Kley¹

¹ Institut für Astronomie & Astrophysik, Universität Tübingen, Auf der Morgenstelle 10, D-72076 Tübingen, Germany

² Max-Planck-Institut für Astronomie, Königstuhl 17, D-69117 Heidelberg, Germany

³ Department of Astronomy, Eötvös Loránd University, Pázmány Péter sétány 1/A, H-1117 Budapest, Hungary

Received 20 December 2007 / Accepted 13 February 2008

ABSTRACT

Context. The formation of resonant pairs of planets in exoplanetary systems involves planetary migration in the protoplanetary disc. After a resonant capture, the subsequent migration in this configuration leads to a large increase of planetary eccentricities if no damping mechanism is applied. This has led to the conclusion that the migration of resonant planetary systems cannot occur over large radial distances and has to be terminated sufficiently rapidly through disc dissipation.

Aims. In this study, we investigate whether the presence of an inner disc might supply an eccentricity damping of the inner planet, and if this effect could explain the observed eccentricities in some systems.

Methods. To investigate the influence of an inner disc, we first compute hydrodynamic simulations of giant planets orbiting with a given eccentricity around an inner gas disc, and measure the effect of the latter on the planetary orbital parameters. We then perform detailed long term calculations of the GJ 876 system. We also run N-body simulations with artificial forces on the planets mimicking the effects of the inner and outer discs.

Results. We find that the influence of the inner disc can not be neglected, and that it might be responsible for the observed eccentricities. In particular, we reproduce quite well the orbital parameters of a few systems engaged in 2:1 mean motion resonances : GJ 876, HD 73 526, HD 82 943 and HD 128 311. Finally, we derive analytically the effect that the inner disc should have on the inner planet to reach a specific orbital configuration with a given damping effect of the outer disc on the outer planet.

Conclusions. We conclude that an inner disc, even though difficult to model properly in hydro-dynamical simulations, should be taken into account because of its damping effect on the eccentricity of the inner planet. By including this effect, we can explain quite naturally the observed orbital elements of the pairs of known resonant exoplanets.

Key words. Accretion, accretion discs - Planets and satellites : formation - Celestial mechanics

1. Introduction

The orbital evolution of a system consisting of very young protoplanets is governed by disc-planet and mutual gravitational interactions. In case of differential migration the semi-major axis ratio of two planets varies with time and - in the situation of convergent migration - capture in a resonant configuration may occur. Indeed, a large fraction of the observed multi-planet systems contain a pair of planets engaged in a resonance. Here, we are interested in mean motion resonances (MMR) where the ratio of the (mean) orbital periods of the outer to the inner planet equals that of two small integers. Among the 6 systems known to be in a MMR, 4 have a ratio of 2:1 : GJ 876, HD 82 943, HD 128 311 and HD 73 526. The system discovered first to lie in a 2:1 configuration (GJ 876) is interesting in several aspects. The planets are both very massive (0.56 and 1.94 M_{Jup}), particularly when considering the small mass of the central star of only 0.33 M_{\odot} . The relatively short orbital periods of the planets (≈ 30 and ≈ 60 days) have allowed for very accurate determination of their orbital elements, which are stated in Table 1. In GJ 876 the two outer planets are 'deep' in the 2:1 MMR, i.e. the apsidal lines of the two osculating orbital ellipses are always aligned and librate with very small amplitudes only (so called apsidal resonance or

corotation). As a consequence of the apsidal resonance the planetary eccentricities show only small variations with time. A resonant configuration like that in GJ 876 can only be established through the action of dissipative effects such as disc-planet interaction. In fact, the mere existence of systems engaged in MMRs is one of the strongest indication that planetary migration has indeed occurred during the early evolution of planetary systems.

The first detailed modelling of GJ 876 has been conducted by Lee & Peale (2002a) who performed customised 3-body simulations of a central host star and two planets with additional (dissipative) forces mimicking the effects of disc-planet interaction. In these type of simulations it is assumed that a pair of planets is still embedded in the protoplanetary disc, which consists of an outer disc only while the inner disc (inside of the inner planet) has already been lost through effects like accretion onto star and planets or final evaporation. In such a configuration only the outer planet is in contact with an even further protoplanetary disc and it experiences typically negative Lindblad torques and migrates inward. On the contrary the inner planet has no ambient material and does not feel any disc torque. In terms of the 3-body simulations by Lee & Peale (2002a) this implies additional forces that reduce the semi-major axis and eccentricity of the outer planet, while the inner planet feels only the direct gravitational forces of the star and outer planet. Capture into a resonant configuration can now occur when during the inward migration

the outer planet crosses the location at which the mean orbital periods have a ratio of two small integers.

The eccentricity damping action of the outer disc onto the outer planet is typically parameterised through the migration rate, i.e.

$$\frac{\dot{e}}{e} = -K \left| \frac{\dot{a}}{a} \right| \quad (1)$$

where a and e are the semi-major axis and eccentricity of the planet, respectively, while the constant factor K relates the damping rates. For low mass planets in the linear regime, it is known that the eccentricity damping time scale $t_e = -e/\dot{e}$ is about h^2 times shorter than the migration time scale $t_a = -a/\dot{a}$ (Tanaka & Ward 2004), where h is the aspect ratio of the disc (generally a few percent). This short time scale has been confirmed recently through fully nonlinear hydro-dynamical simulations in 2 and 3 dimensions (Cresswell et al. 2007). Hence, for low mass planets one may safely assume that they migrate inward on nearly circular orbits unless otherwise disturbed by additional objects in the system. For higher planetary masses the value (and also the sign) of K is not known exactly, but due to the opening of a gap it is to be expected that the damping on the eccentricity will be reduced with respect to the linear case. The simulations by Lee & Peale (2002a) indicate now that for values of K equal to unity the resonant action leads to a strong growth of eccentricity of both the inner and outer planets much larger than the observed values ($e_1 \approx 0.03$ and $e_2 \approx 0.22$). Lee & Peale (2002a) pointed out that the final state of the system is determined by K . For a vanishing K , i.e. no eccentricity damping, the planetary eccentricities continue to grow. To match the observations Lee & Peale (2002a) had to assume a value of $K = 100$, a value that appears to be very large considering the high masses of the planets.

The convergent migration of two massive planets has been demonstrated in a variety of hydro-dynamical simulations (Kley 2000; Bryden et al. 2000; Snellgrove et al. 2001; Papaloizou 2003). Through multi-dimensional hydro-dynamical simulations of resonant planetary systems it has been shown that for masses in the Jupiter regime the value of K lies around 1 – 10 at most (Kley et al. 2004), and in a detailed study of the system GJ 876, Kley et al. (2005) have shown that in hydro-dynamical simulations where the inner disc has been depleted the final eccentricities of the planets will always be much larger than the observed values unless one assumes that the outer disc dissipates rapidly on the viscous time scale. Hence, this scenario does not allow for the migration of the resonant planets over a larger radial distance. While in hydro-dynamical simulations of discs with embedded planets it is often found that the inner disc is depleted rapidly, this may in reality not be the case and be an artefact of inappropriate inner boundary conditions. As shown by Crida & Morbidelli (2007), even in the presence of a planet an inner disc will survive for much longer than found previously. In this situation it can be expected that the inner disc will have a dynamical influence on the inner planet and induces possibly some additional damping of the eccentricity. The influence of such an eccentricity damping of the inner planet was mentioned first by Lee & Peale (2002a) for the particular case of GJ 876. They found that a value of $K = 10$ for both planets yields final eccentricities in the observed range. The first full hydro-dynamical study in this direction – including an inner disc – was done for the resonant system HD 73 526 by Sándor et al. (2007); in their study, they have shown that the inclusion of an inner disc indeed leads to an additional eccentricity damping of the inner planet,

and allows more extended radial migration with reasonable final eccentricities.

In this paper we analyse this effect in more detail and investigate the dynamical influence that an inner disc has on a planet. In Sect. 2 we perform a sequence of hydrodynamic simulations and measure the torque and power exerted by the disc on the planet and evaluate the change in eccentricity and semi-major axis as a function of the planetary eccentricity. In Sect. 3 we perform a full time evolution of a pair of planets embedded in a proto-planetary disc for realistic parameters with specific application to GJ 876. We show that the torque and the power generated by the inner disc yield an effective damping of e which results in moderate final eccentricities even for extended radial migration. Last, in Sect. 4, we apply an eccentricity damping to the inner planet, in the frame of N-body simulations with artificial non-conservative forces to mimic the effect of the disc. We apply this to a few exoplanetary systems, and try to recover the observed orbital elements with a realistic migration scenario. Sect. 5 summarizes our results.

2. Effect of a gaseous inner disc on the orbital elements of a planet on an eccentric orbit

To measure the influence that an inner disc has on the orbital elements of a planet orbiting around it on an eccentric orbit, we perform a suite of hydro-dynamical simulations. Here the disc is treated as a two-dimensional gas that lies in the orbital plane of the planet. The disc material is (basically) only present inside the planetary orbit, so that the effect of the inner disc can be isolated. The planet has a mass $M_p = 2.14 \times 10^{-3} M_*$ and has a fixed orbit with semi major axis $a = 1$, and a given eccentricity e , that changes from one simulation to another.

The disc is treated as a non-self-gravitating gas that nevertheless can interact gravitationally with the planet. From the expressions for the planetary energy $E = -G(M_* + M_p)M_p/2a$ and angular momentum $H = M_p \sqrt{G(M_* + M_p)a(1 - e^2)}$, one can easily derive :

$$\dot{a}/a = -\dot{E}/E \quad (2)$$

$$\dot{e}/e = \frac{e^2 - 1}{2e^2} \left(\frac{\dot{E}}{E} + 2 \frac{\dot{H}}{H} \right) \quad (3)$$

In the present simulations we keep the orbit of the planet fixed but monitor the torque (\dot{H}) and power (\dot{E}) acting on the planet (averaged over one orbit). We have checked that if the planet is released from its fixed orbit, its eccentricity and semi major axis follow the expected evolution.

The code we use is FARGO, by Masset (2000a,b) which is a 2D hydro-code using cylindrical coordinates (r, φ) with an isothermal equation of state. Thus, the sound speed is given by $c_s = hr\Omega$, where Ω is the local angular velocity, r is the distance to the central star, and h is the aspect ratio, which is here 0.05. The gas viscosity ν is given by an α -prescription ($\nu = \alpha c_s hr$, Shakura & Sunyaev 1973), with $\alpha = 10^{-2}$. The grid covers the region from 0.4 to 1.62 in radius, divided in 112 elementary rings (logarithmically spaced), themselves divided in 500 sectors. The inner boundary condition is non-reflecting. More precisely, at every time step the density in the zeroth ring is set equal to the one in first ring, rotated by a suitable angle to mimic wave propagation, which avoids wave reflection; then, the density in the zeroth ring is shifted such that the azimuthally averaged density is the same as initially. The outer boundary is open, which means that outflow of gas out of the grid is permitted.

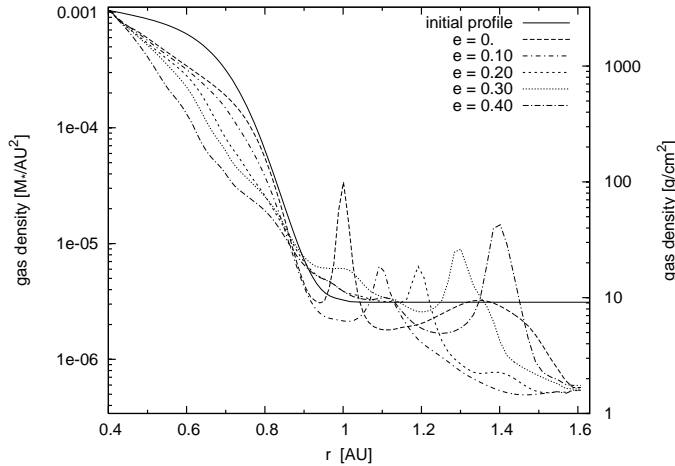


Fig. 1. Gas density profiles after 400 orbits for a few planet eccentricities, and common initial profile (plain line).

The coordinate system is centred on the star. It can be non-rotating, corotating with the planet, or rotating at a constant angular velocity with a period equal to that of the planet

$$\Omega_0 = \left(\frac{G(M_* + M_p)}{a^3} \right)^{1/2}. \quad (4)$$

Even with the FARGO algorithm, which at each ring transforms essentially to a corotating frame, the choice of a different rotation rate of the coordinates may change the gas dynamics close to the planet. We have performed comparison simulations in all three frames and display some results below. In the corotating frame, gas in the Hill sphere simply rotates around the planet, whose motion is only radial from apoastron to periastron and back. In the non-rotating frame, the motion of the planet around the star in the grid tends to spread artificially the Hill sphere. For large eccentricities, however, the corotating frame is not advantageous because it is not rotating at a constant angular velocity, which implies additional terms in the equations of motion. Therefore we prefer the last option, a frame rotating with the constant speed Ω_0 in which the planet describes an epicycle.

The initial density profile corresponds to an approximate gap opened by the planet, without the outer disc, so that an equilibrium profile and a stationary regime are quickly reached. The initial profile can be seen on Fig. 1 as a solid line. The initial total mass of gas in the disk is $1.53 \times 10^{-3} M_* = 71\% M_p$. The final density profiles after 400 orbits for various planet eccentricities are also displayed on Fig. 1. The profiles are taken when the planet is at apoastron, and the density spike at $r = 1 + e$ corresponds to the Hill sphere of the planet. The larger the eccentricity, the more depleted the inner disc. The outer disc is clearly empty. In the 5 presented cases, the simulation has been run in the non-rotating frame.

2.1. Average effect of the inner disc

The power and the torque from the disc on the planet become almost constant after about 200 orbits in most cases, and we measure them after 400 orbits. In the measure of the force exerted by the gas on the planet, we exclude material in the Hill sphere, using a tapering function given by :

$$f(d) = \left[\exp\left(-\frac{d/r_H - p}{p/10}\right) + 1 \right]^{-1} \quad (5)$$

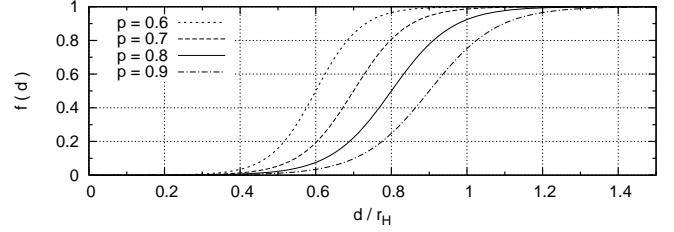


Fig. 2. Tapering function $f(d)$ defined by Eq. (5) for four values of the parameter p .

where d is the distance to the planet and r_H is its Hill radius $r_H = r_p(M_p/3M_*)^{1/3}$ (r_p being the distance between the planet and the star); p is a dimensionless parameter set equal to 0.8. This function is plotted on Fig. 2 for different values of p . We stress that the use of such a tapering is really important as the gas close to the planets exerts on it a strong force, which should not be taken into account because this gas is gravitationally bound to the planet and should be considered as a part of it. With self-gravity, this gas should feel the same force as the planet and naturally follow it; using a tapering frees the planet from carrying artificially this material. The influence of the shape of the tapering function will be discussed below.

The results are shown in Fig. 3 for the three above mentioned options for the rotation rate of the coordinate system. The quantities are normalised by $\mu = M_{\text{disc}}/M_p$, because the force felt by the planet is proportional to the gas density. The two top panels display the influence of the inner disc on the orbital elements e and a . For $e \geq 0.1$, the eccentricity is effectively damped on a time scale of about two thousands of orbits, as can be seen in the bottom left panel displaying $\tau_e = -e/(\dot{e}/\mu)$; the dispersion in the values of τ_e for $0.1 \leq e \leq 0.15$ is simply due to the fact that \dot{e} is close to zero. This confirms the idea by Lee & Peale (2002b) and Sándor et al. (2007) that an inner disc has indeed a damping effect on the planetary eccentricity. For low eccentricities ($e \leq 0.1$), the influence of the disc is small ($|\dot{e}| < 4 \times 10^{-5}$ orbit $^{-1}$), and could even lead to a small excitation of the eccentricity.

It is well-known that a planet on a circular orbit exerts a negative torque on the inner disc (Lin & Papaloizou 1979; Goldreich & Tremaine 1980). It repels the gas, leading to the opening of a gap. When the density gradient at the gap edge is steep enough, an equilibrium arises (see for instance Crida et al. 2006). Then, the planet feels a positive torque from the inner disc. For $e = 0$, we find that the planet feels a positive torque (which is equal to the power), as expected; consequently, $\dot{a} > 0$. But as e increases, the power decreases, and for $e \gtrsim 0.3$, the semi major axis variation expected if one releases the planet is negative (top right panel). In a sense, the inner disc attracts the planet more and more as the eccentricity grows.

As a consequence of the variations of \dot{a} and \dot{e} with e , the simple modelling given by Eq. (1) with K constant seems to be an over simplification. The bottom right panel of Fig. 3 displays $(\dot{e}/e)/(\dot{a}/a) = K$ as a function of e . It varies a lot. The dispersion around $e = 0.3 - 0.35$ is due to the change of sign of \dot{a} . For $0.1 < e < 0.25$, a K factor of the order of minus a few seems reasonable, but a precise value can not be stated. However, it is clear that the effect of the inner disc on the planet can not be neglected. In particular the left panels show that a significant damping of the eccentricity has to be taken into account.

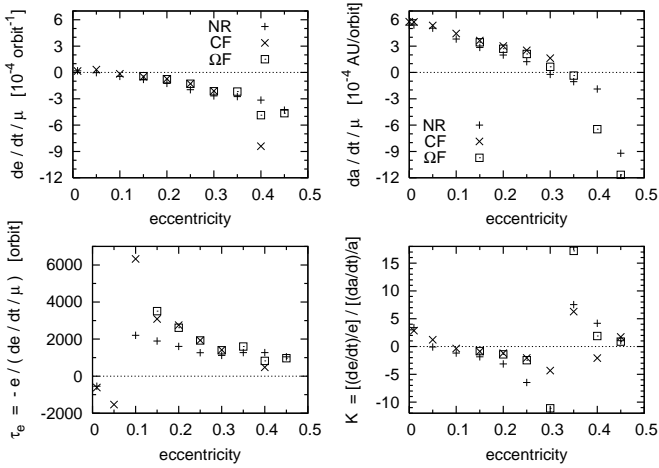


Fig. 3. Influence of the inner disc on a planet on a fixed orbit, as a function of the eccentricity. NR (+ symbols): in the non-rotating frame; CF (x symbols): in the corotating frame; ΩF (open squares): in the frame rotating monotonically with the same period as the planet.

2.2. More detailed analysis

To investigate the physical mechanism more thoroughly, we focus on the case where $e = 0.15$ and where the frame is rotating at a angular constant velocity Ω_0 . On Fig. 4, we plot the specific torque and power felt by the planet during one orbit, starting at apoastron. The units are normalised such that $a = G = M_* = 1$, and thus $\Omega_0 = \sqrt{1.00214}$. Four curves are presented, corresponding to measures on the same orbit with four different values of the parameter p in Eq. (5), in the range $[0.6; 0.9]$. The larger the p factor, the smaller the amplitude of the oscillation. This oscillation is due to gas in the Hill sphere. For each case, the average is plotted as a straight horizontal line. Both the mean torque and power vary by 10 percent with varying p . So does the corresponding \dot{a} , while \dot{e} varies by about 5%.

A fifth curve, labeled $p = 0$, is drawn on each panel of Fig. 4 which corresponds to the case where $f = 1$ (no tapering). Under these conditions, with an eccentric orbit and an irregular, non-stationary density structure (also within the Hill sphere), the measured torque and power are quite different, and somehow noisy. The amplitude excursions are so large (into the negative) that the mean values for the $p = 0$ case, averaged over one orbit, give $\dot{a}/\mu = -10^{-3}$ instead of 2.8×10^{-4} with $p = 0.8$, and $\dot{e}/\mu = -7.14 \times 10^{-4}$ instead of -7.95×10^{-5} . This clear difference of the $p = 0$ case, and the very good agreement between the other four cases $p \in [0.6; 0.9]$, enlightens the importance and necessity of tapering.

For a better understanding of the process, on Fig. 5 are drawn in the frame rotating at constant angular velocity Ω_0 the traces during one orbit of the vectors \mathbf{r}_p , $\mathbf{v}_p|_{\text{NR}}$, $\mathbf{v}_p|_{\Omega F}$, and \mathbf{F} (respectively the position of the planet, its velocity in the non-rotating and rotating frames, and the force it feels from the disc), in the normalised units. The force is measured with $p = 0.8$ and is magnified by a factor 5×10^6 for visibility. The vectors are drawn at the beginning of the orbit; then, every twentieth of orbit, a cross symbol is drawn on the curve. In the frame rotating at the velocity Ω_0 , the planet describes an epicycle centred on $(x = 1, y = 0)$, in the clockwise direction starting at $(x = a + e = 1.15, y = 0)$. The planet velocity describes also an epicycle, centred on $(v_x = 0, v_y = a\Omega_0)$, in the anti-clockwise direction, starting at $(v_x = 0, v_y < 1)$; the velocity in the rotating

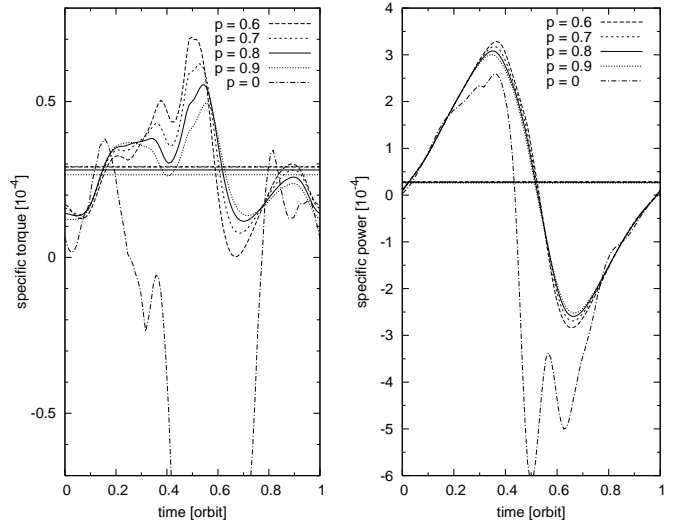


Fig. 4. Specific torque (left panel) and power (right panel) acting on the planet during one orbit for a fixed semi-major axis and eccentricity, $e = 0.15$. The different curves correspond to measures using different values of the p parameter in Eq. (5). The horizontal lines correspond to the average in each of the four cases $p \neq 0$.

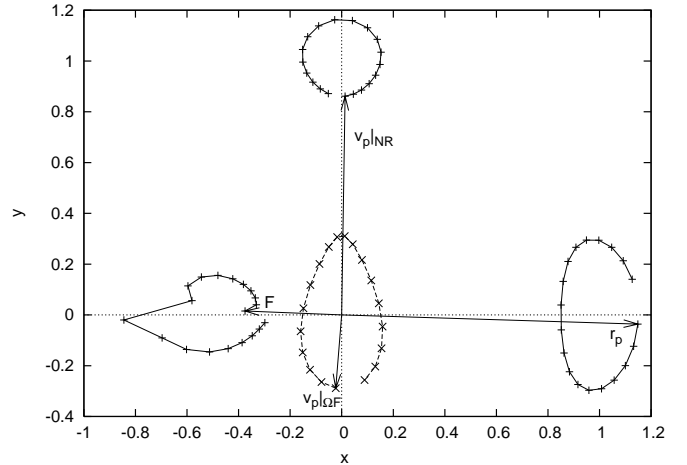


Fig. 5. Evolution during one orbit of the vectors \mathbf{r}_p : position of the planet in the frame rotating at velocity Ω_0 (right); $\mathbf{v}_p|_{\text{NR}}$: velocity of the planet in the non-rotating frame (top); $\mathbf{v}_p|_{\Omega F}$: velocity of the planet in the frame rotating at constant velocity Ω_0 (middle); \mathbf{F} : force from the disc on the planet (left, arbitrary unit).

frame $\mathbf{v}_p|_{\Omega F}$ is plotted as a dotted line, describing a curve around zero in the clockwise direction. As could be expected, the force felt by the planet is directed toward the inner disc ($F_x < 0$), more precisely in the direction of the wake. The wake tends to rotate at a constant velocity. So, between apoastron and periastron, when y_p is negative (the planet is late with respect to the average rotation at speed Ω_0), the wake leads the planet and F_y is positive. After periastron, the planet leads the root of wake, $y_p > 0$ and $F_y < 0$. This can be seen on the density maps of Fig. 6. This explains the variations of the sign of the power $\mathbf{v}_p|_{\text{NR}} \cdot \mathbf{F}$ observed in Fig. 4. The torque $\mathbf{r}_p \wedge \mathbf{F}$ is always positive because the angle $(\mathbf{r}_p, \mathbf{F})$ always remains slightly smaller than π , as can be checked on the figure.

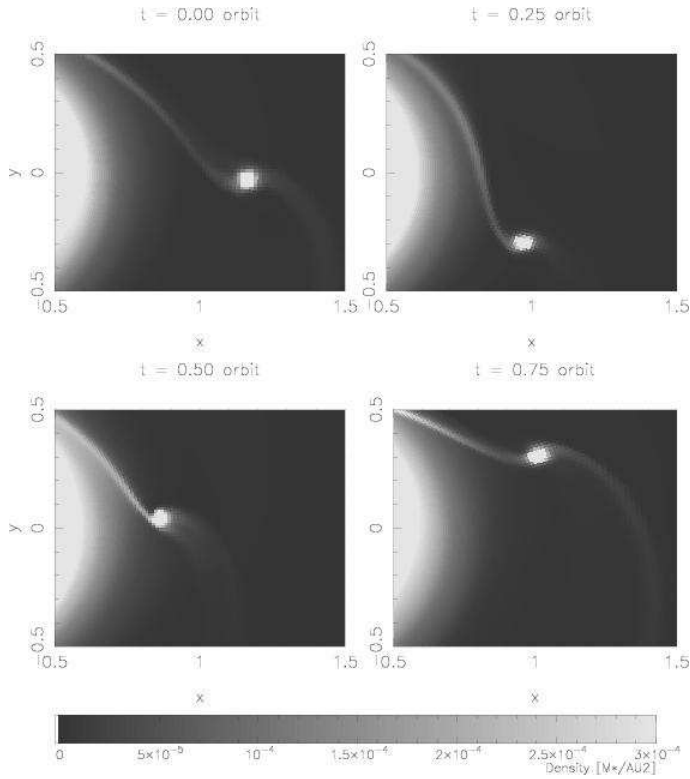


Fig. 6. Density maps, in linear grey scale, in the frame rotating at constant velocity Ω_0 at four different moments of the orbit corresponding to Fig. 4.

2.3. Discussion

In this section, we have treated only a particular case, with a given planet mass and given disc parameters. The width, the depth and the shape of the gap opened by the planet would change if the disc viscosity, aspect ratio, or the planet mass vary, and the inner disc effect would consequently differ. Also, some numerical issues, like the smoothing length for the potential, the tapering, and the choice of the frame can affect the measured force from the gas on the planet, from a quantitative point of view. As seen from the right panel of Fig. 4 a small change in the power, e.g. due to numerical aspects, may possibly lead to a sign reversal of the average value (implying a reversed migration). Exploring all the parameter space would be prohibitive and is beyond the scope of this paper. We simply wanted to demonstrate here that the inner disc has a non negligible damping effect on eccentric giant planets, and we provide a qualitative explanation of this phenomenon.

During the evolution towards the final equilibrium state the mass of the disc is decreasing. At the end of the simulations it lies between 30 and 50 percent of the planet mass in all cases. Then the question arises whether one could have some eccentricity excitation in the disc induced by the planet through a tidal instability mechanism operating through the inner 3:1 Lindblad resonance in the disc (Lubow 1991). In case of the inverse situation, i.e. a planet orbiting *inside* an outer disc, it has been shown that for sufficiently large planet masses ($M_p \gtrsim 3M_{\text{Jup}}$) the outer disc will turn eccentric even in case of a planet on a circular orbit (Papaloizou et al. 2001; Kley & Dirksen 2006). The strength of such a mechanism scales inversely with the planet mass such that for the smallest planet masses the timescale of eccentricity growth is several thousand planetary orbits. For the instability to work the gap created by the planet must be wide enough such

The GJ 876 planets.

name	$M \sin i$ (M_{Jup})	period (days)	a (AU)	e
b	1.935	60.93 ± 0.03	0.20783	0.029 ± 0.005
c	0.56	30.38 ± 0.03	0.13	0.218 ± 0.002
d	0.023	1.94	0.020807	0.

Table 1. Parameters of the system GJ 876 as given by Laughlin et al. (2005) for GJ 876b and GJ 876c, and by <http://exoplanets.eu/> for GJ 876d.

that the outer 2:1 Lindblad resonance, which damps eccentricity, has been cleared. Adding a small planetary eccentricity will reduce the necessary planet mass slightly (D’Angelo et al. 2006).

To check for this effect in our simulations we have continued models for $e = 0.15$ for over 3500 orbits and have not seen any indication for eccentricity growth in the disc, even in a test case where the planet mass has been increased to $5M_{\text{Jup}}$. We can conclude that for our planet masses we do not expect an eccentric inner disc. Anyway, our simulations have clearly reached a steady state when we measure the torque and power of the force of the inner disc on the planet, and we expect eccentricity damping of the planet by the nearly circular disc. As pointed out above, we checked this behaviour through simulations where we release the planet from its fixed orbit and follow its orbital evolution self consistently. Here we find exactly the predicted results for the change in a and e of the planet.

The non occurrence of an eccentric inner disc can be explained by the effect that due to the small mass of the planet and the not small viscosity and pressure, not all the eccentricity damping resonances in the disc are cleared, even for the large eccentricities of the planet.

3. Application to the GJ 876 system

3.1. Characteristics of the system

GJ 876 is a $0.32M_{\odot}$ M4 star that hosts 3 planets, the two largest of them being in a 2:1 Mean Motion Resonance (MMR), see Table 1. The resonant angles that characterise this resonance are $\theta_1 = \lambda_c - 2\lambda_b + \omega_c$, $\theta_2 = \lambda_c - 2\lambda_b + \omega_b$, and $\Delta\omega = \omega_b - \omega_c$, where λ is the mean longitude and ω is the longitude of the periastron. They all three librate around 0° . Laughlin et al. (2005) estimated the amplitude of their librations: $|\theta_1|_{\text{max}} = 7 \pm 1.8^\circ$, $|\theta_2|_{\text{max}} = 34 \pm 12^\circ$, and $|\Delta\omega|_{\text{max}} = 34 \pm 12^\circ$.

Like all the hot Jupiters, the two giant planets in GJ 876 most likely formed further out in the protoplanetary disc (beyond the snow-line, where water is solid and can contribute to the formation of a massive core) and then migrated toward the central star. Migration is also supported by the resonant motion: such a configuration can only be reached by convergent motion of the planets. Thus, the outermost planet must have been migrating inward faster than the innermost one and eventually captured it in resonance; or both planets may have been orbiting in a common gap in the disc, repelled one onto the other by the inner and outer discs. Then, they can migrate together in this configuration until their current position. Dissipation in the gas disc can also modify the amplitude of libration of the resonant angles.

The migration of two giant planets in MMR in a gas disc has been studied first by Masset & Snellgrove (2001) for the case of Jupiter and Saturn, and in more details by Morbidelli & Crida (2007). They showed that if the outermost planet is significantly lighter than the innermost one, the migration of both planets may well be stopped or reversed outward. In our case of GJ 876 the

outer planet is substantially more massive than the inner one, so that we expect an inward migration of the pair of planets. Under this consideration, the observed small semi-major axes of GJ 876b and GJ 876c are not a surprise. However, the innermost of the two resonant planets (GJ 876c), being pushed inward by the outer one (GJ 876b), should have its eccentricity dramatically raised, according to N-body simulations with artificial migration rate and detailed hydro-dynamical simulations, as discussed in the Introduction. But we have seen that an inner gaseous disc has a damping effect on the eccentricity of a giant planet, at least for $e \geq 0.1$. Thus, we suggest that the presence of a gaseous disc inside the orbit of GJ 876c could prevent its eccentricity from reaching unreasonable large values. To verify this hypothesis, below we compute numerical simulations of the GJ 876 system embedded in a disc, using a hydro-code.

3.2. Code description and numerical parameters

Numerical scheme : To have the whole disc simulated, we used the code by Crida et al. (2007), derived from FARGO by Masset (2000a,b). A 2D polar grid covers the region where the planets orbit, surrounded by a 1D grid that extends over all the disc, the disc being assumed axisymmetrical far from the planets. As pointed out in Crida et al. (2007), this 1D grid enables us to take into account the global disc evolution, which governs the type II migration of the giant planets. In addition, the inner disc evolution is self-consistently computed down to an arbitrarily small inner radius, that could not be reached by a 2D grid for numerical reasons. Thus, the planets can feel the influence of a realistic inner disc. Consequently, this code is well adapted to the problem that we wish to study.

In contrast to the previous calculations where we have used a non-inertial frame centred on the star, the usage of the added 1D-grid requires that the frame is inertial and centred on the centre of mass of the system (here : star + planet + disc).

The tapering function used here is f as given in Eq. (5), with $p = 0.6$.

The 2D grid spans over the region where the planets orbit : $r \in [0.055 ; 0.655]$, with a resolution of $N_s = 500$ sectors in azimuth and $N_r = 300$ rings in radius; the rings width is thus $\delta r = 0.002$ AU, which also applies for the 1D grid. The outer edge of the 1D grid is arbitrarily fixed at $r = 10$ AU, which is far enough. The inner edge will be discussed below.

Disc parameters : The damping effect of the inner disc is proportional to its mass, in particular to the gas density and the amplitude of the wake close to the planet. The deeper the gap opened by the innermost planet, the smaller the wake there. The wider the gap, the further the disc lies from the planetary orbit. Consequently, a larger gap leads to a smaller damping. The shape of the gap is determined by the gas parameters ν and h (Crida et al. 2006). Thus, these parameters play a crucial role for the damping as well. Here, the gas viscosity is still given by an α -prescription, with $\alpha = 10^{-2}$. The chosen aspect ratio is $h = 0.07$.

Radius of the inner edge of the disc: Crida & Morbidelli (2007) have shown that the inner disc evolution is strongly dependent on the radius of the inner edge of the disc, and more precisely on the ratio between this radius and the radius of the planetary orbit. Generally, this radius is poorly constrained, and strongly model-dependent. So, the mass of the inner disc could

be very uncertain : shall this radius be close to 0.13 AU, and there would be no inner disc in GJ 876 ; shall it be close to the stellar radius and there would be room for a massive inner disc.

Fortunately, in the case of GJ 876, a ‘hot Neptune’ is present at 0.02 AU. This gives a strong constraint for the location of the inner boundary. Indeed, the migration of this planet stopped there for some reason.

A first possibility is that this planet, not massive enough to open a gap, and thus migrating in the type I regime, was caught in a planet trap (Masset et al. 2006). This planet trap could be the inner edge of the disc : indeed at this location, the disc density increases rapidly from zero, leading most probably to a positive gradient of the vortensity and a strong corotation torque. Then, the radius of the inner edge of the disc should have been close to 0.02 AU.

A second possibility is that GJ 876d migrated inwards in the gas disc until it lies in the empty cavity inside the edge of the disc. A few reasons may explain that this planet crossed the planet trap created by the disc edge. The trap may not have been strong enough (a jump in density over a only few scale heights of the disc is required) ; also, the aspect ratio and the viscosity of the disc may have been so low at this place that this planet could perturb the disc profile destroying the trap. Finally, turbulence in the disc causes random torques, helpful to jump the trap. Once the planet is in the cavity, it feels a negative torque from the disc at outer Lindblad resonances (Goldreich & Tremaine 1979, 1980). Thus, the planet goes on migrating inward until there is no more gas at the location of its 2:1 resonance (the outermost one). In that case, the inner edge of the disc must have been located at the 2:1 resonance with GJ 876d, that is at 0.033 AU. Then, as the disc is evaporated by the star from inside out, the planet remains there.

Let us focus on this second possibility. We claim that the inner disc could not extend further inward than 0.033 AU, otherwise it would have pushed GJ 876d inward, and that it should have extended exactly down to this radius, otherwise there would be no reason for GJ 876d to migrate inward to its present position. Thus, the open inner edge of the 1D grid will be located at $r = 0.033$ in our simulation.

3.3. Results

The innermost planet, GJ 876d, is not computed. The two largest ones are launched on circular orbits at $r = 0.36$ and 0.21 AU respectively. At first, the planets influence each other and influence the disc, but do not feel the disc effect. So, the planets shape a gap in the density distribution and the gas disc reaches an equilibrium for this planetary configuration. This phase lasts for 75 years, which makes about 200 orbits for the outer planet. The initial density profile as well as the profile at this time are shown on Fig. 7 ; the final density profile is also plotted. The mass of gas present in the 2D grid after this first phase is 2.69×10^{-2} stellar mass ($\sim 1.7 \times 10^{28}$ kg).

Then, the planets are released and allowed to move under the influence of the gas. The evolution of their orbital elements is shown on Fig. 8. As expected, the outer planet migrates inward, pushed by the outer disc (curve labelled a_2 on Fig. 8). However, the inner planet also migrates inward, although less rapidly. This is because it did not open a very clean gap (see Fig. 7) and it lies on the inner edge of the gap opened by GJ 876b ; consequently the inner planet feels a strong negative corotation torque.

The 3 relevant resonant angles associated with the 2:1 resonance are shown on Fig. 9. After ~ 110 years, the outer planet catches the inner one in its 1:2 Mean Motion Resonance (θ_1 ,

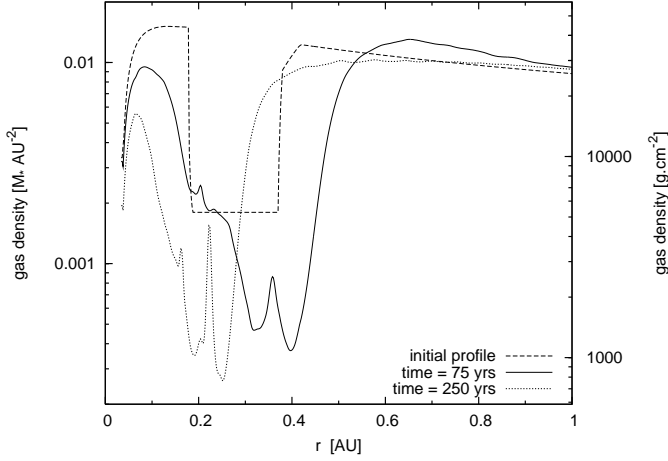


Fig. 7. Density profiles at time 0 (dashed line), at the moment where the planets are released (solid line), and at the end of the simulation (after 250 years, dotted line).

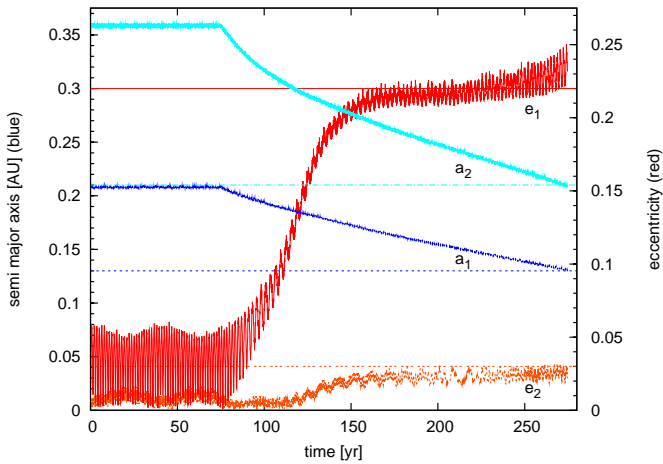


Fig. 8. Semi major axis (blue, left y-axis) and eccentricity (red, right y-axis) evolution of GJ 876b (light colour, a_1 , e_1) and GJ 876c (dark, a_2 , e_2). The horizontal lines correspond to the observed values, as given by Table 1.

θ_2 and $\Delta\omega$ start librating around 0° with small amplitude), and the pair of planets goes on migrating in this configuration. The eccentricities rise, as expected. But after a phase of eccentricity growing, a limit value is reached for e_1 and e_2 at about 150 years. The planets go on migrating at the same rate, while their eccentricities remain constant. The value obtained for the eccentricities is very close to the one given by Laughlin et al. (2005). After ~ 270 years, the planets have reached their present semi major axes, and their eccentricities are oscillating in the ranges $0.019 < e_2 < 0.032$ and $0.21 < e_1 < 0.25$. The amplitude of the libration of the resonant angles at this point are $|\theta_1|_{\max} \approx 18^\circ$ (but it was about 8° at 220 years), $|\theta_2|_{\max} \approx 28^\circ$, and $|\Delta\omega|_{\max} \approx 20^\circ$. These amplitudes are somewhat larger than the ones given by Laughlin et al. (2005), but the agreement for the semi majors axes and eccentricities is excellent.

3.4. Discussion

Role of the inner disc: For comparison, the same simulation has been run with no action of the disc on the inner planet. The

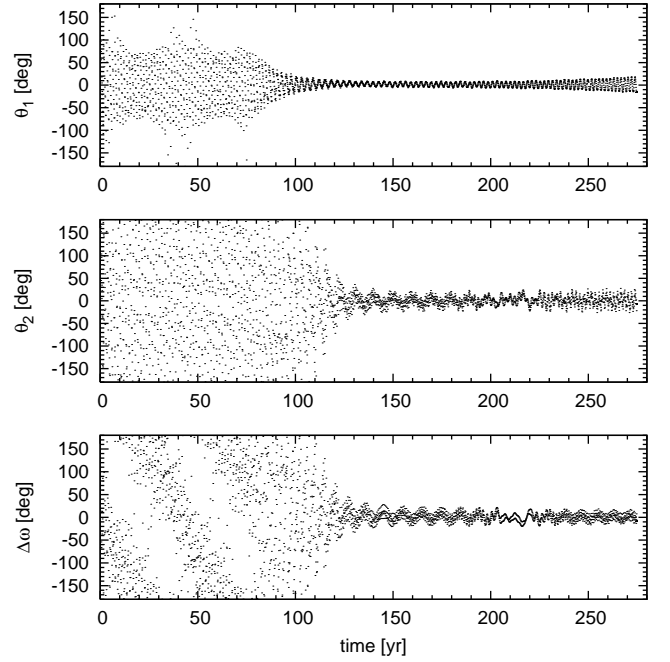


Fig. 9. Resonant angles associated with the 2:1 resonance θ_1 , θ_2 , $\Delta\omega$ as functions of time.

semi major axis evolution of the two planets is almost not affected; indeed migration is dominated by the outermost planet, which is pushed inward by the outer disc, and that pushes inward the inner planet through the resonance locking. Consequently, the curves of $a_i(t)$ overlap the ones of Fig. 8. On the contrary, the behaviour of the eccentricity of the inner planet e_1 changes dramatically. It increases faster and continuously, as expected from N-body simulations. In fact, both eccentricities rise up to high values that are not compatible with the observations ($e_1 \sim 0.45$, $e_2 > 0.1$). The eccentricities evolution is displayed on Fig. 10 for the previous case (labelled “ref”), and in the case where the action of the disc on the inner planet is switched off (labelled “no inn.”). This convincingly shows the very important role of the inner disc in eccentricity damping for the inner planet, which in turn affects the eccentricity of the outer one as well.

Role of the tapering function: We should also mention that in the standard simulation, if one takes $p = 0.8$ instead of 0.6 in the tapering function f (see Eq. (5) and Fig. 2), the inner planet reaches a higher limit eccentricity (between 0.275 and 0.3), while the eccentricity of the outer one saturates between 0.035 and 0.05. The eccentricities evolution in this case is also displayed on Fig. 10 (curves labelled “ $p = 0.8$ ”). The eccentricities still do not reach extremely high values thanks to the disc damping, but this is not in very good agreement with the observations (horizontal lines on the figure), especially for what concerns the inner planet. This also shows that the tapering function can have an influence on the final eccentricity of the planets in numerical simulations (as could be expected from Fig. 4), and one should take this into consideration.

Disc dispersal: To match with the present state, one has to disperse the disc when the planets have reached their present semi-major axis (at time $t \sim 270$ yr). This is a common problem when modelling the extra-solar planets.

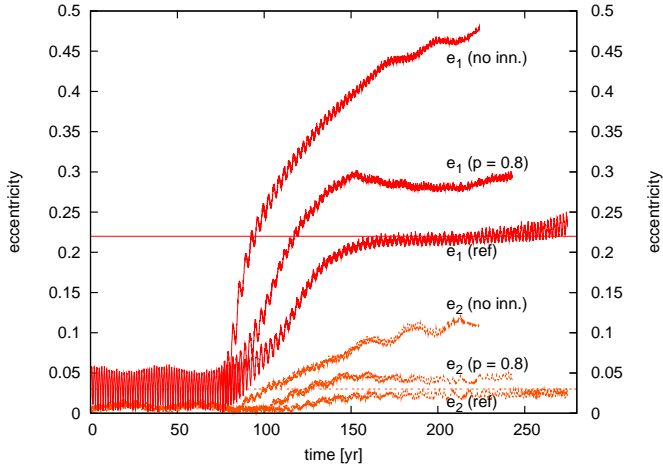


Fig. 10. Eccentricity evolution of GJ 876 b (light colour, e_2) and GJ 876 c (dark, e_1) in three cases: (i) standard simulation (same as Fig. 8, curves labelled “ref”); (ii) same as (i) but the inner planet is not affected by the disc (curves labelled “no inn.”); (iii) same as (i) but the p parameter of the tapering function f is 0.8 (curves labelled “ $p = 0.8$ ”). The horizontal lines correspond to the observed values, as given by Table 1.

To check what happens when one removes the gas disc, we applied a procedure also used in Morbidelli et al. (2007) and Thommes et al. (2007) to have the gas disappear smoothly for the planetary system not to be perturbed by a sudden change in the potential: from time $t = 250$ yr, the gas density is decreased exponentially in each cell of the grid with a time scale of 27.5 years. The result is shown on Fig. 11: as the gas disappears, the planets remain in 2:1 MMR, while their migration speed decreases exponentially (it is well known that when the planet is more massive than the disc, the inertia of the planet is the limiting factor in the type II migration regime). One should note in passing that as the migration speed and the eccentricity damping are both proportional to the gas density, the K factor is not affected in this procedure; consequently, the equilibrium value of the eccentricities is not affected, and they remain close to 0.03 and 0.22 respectively, while the semi major axes converge to 0.21 and 0.13 AU. In the end, gas has almost completely disappeared, and we are left with a planetary system very similar to GJ 876.

The disc clearing process is complex and not well constrained, in particular in the vicinity of the star. In general, the gas density first slowly decreases while the disc accretes onto the central star and spreads outward. When the density is low, the photo-evaporation by the central star can play a significant role and erode the disc. The extreme UV photons ionise and heat the upper layer of the disc, so that gas can leave the potential well of the star, and the density decreases. However, this works more efficiently at radius larger than about 1 AU (close to the star, the gravity is too strong). Consequently, the region where the two giant planets of GJ 876 are orbiting should not be much affected; in particular, the inner disc should not disappear. The remnant disc inside ~ 1 AU will viscously spread onto the star and out. So, the migration path of the planets should not be much affected. In addition, the viscous evolution dominates the disc evolution until the density is very low. Then, photo-evaporation happens on a timescale that is much shorter than the disc life time. Thus, the final phase of gas dispersal occurs when the disc

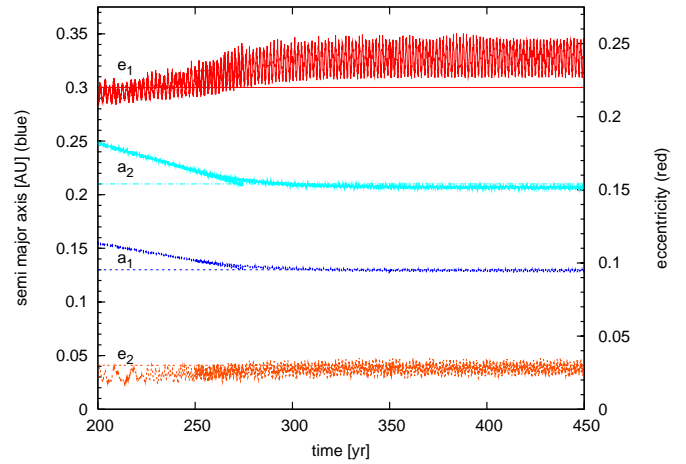


Fig. 11. Semi major axis and eccentricity evolution of GJ 876 b and GJ 876 c, with disc clearing from time $t = 250$ yr on. The horizontal lines correspond to the observed values, as given by Table 1.

is too low to have any significant influence on the planets on such a short timescale.

Thus, we think that the planetary configuration should not be significantly perturbed during this phase, and that the above modelling by exponential damping of the density gives reliable results. Anyway, these planets somehow migrated toward their host star, until the gas density was too low to push them. They were left at 0.13 and 0.21 AU, and then the disc disappeared. Our simulation shows that when the planets stop migrating, they automatically have the correct eccentricities; hence, our simulation is consistent with the observed configuration. To our knowledge, this is the first time that an extra-solar system is reproduced in a fully hydro simulation taking into account all the protoplanetary disc and allowing for a significant migration of the planets with correct eccentricities.

4. Modelling an inner disc by N-body calculations

Studying the effect of an inner disc on the evolution of the resonant planetary systems by full hydro-dynamical calculations (as done in the previous section) requires typically a large amount of computer time. Fortunately, the effects of the outer and inner discs can also be modelled approximately conveniently by gravitational N-body simulations using properly parameterised non-conservative forces. These forces can be derived by using the migration rate \dot{a}/a and the eccentricity damping rate \dot{e}/e of a planet embedded into the protoplanetary disc (see Lee & Peale 2002a; Beaugé et al. 2006, for two different approaches). Instead of the migration and damping rates one can also use the corresponding e -folding times defined as $\tau_a = -(\dot{a}/a)^{-1}$ and $\tau_e = -(\dot{e}/e)^{-1}$.

When studying the formation of a resonant system consisting of an inner and an outer giant planet, usually the outer planet is forced to migrate inward. When the ratio of their semi-major axes approaches a critical limit, a resonant capture may take place between them (for the conditions of a resonant capture into the 2:1 MMR see Kley & Sándor 2007). After the resonant capture the two planets migrate inward as the outer one still feels the negative tidal torques of the disc.

Having studied in the previous section the hydro-dynamical evolution of GJ 876 thoroughly, in this section we provide further results obtained in the framework of the three-body problem

with dissipative forces. Our results show that the presence of an inner disc during the migration of the giant planets is consistent with the observed state of the resonant systems having two giant planets engaged in a 2:1 MMR.

Since the eccentricity of the inner planet is excited by the resonant interaction, its orbit becomes more and more elongated penetrating into the inner disc. This represents a damping mechanism which acts against the eccentricity excitation, and may set a quasi-equilibrium between these processes keeping the eccentricity of the inner planet on a constant value (within certain limits) during the whole migration process. The effect of an inner disc can be investigated by using a repelling non-conservative force acting on the inner planet parameterised by a positive migration rate \dot{a}/a and a negative \dot{e}/e . Similarly to the case of the inward migrating outer planet, a ratio K of the above parameters can also be defined. According to the definition of the e -folding times, τ_a will have a negative sign in this case.

We note, however, that when both the outward and inward migration of the outer and inner planets are considered simultaneously, the final state of the system cannot be characterised uniquely by using only the K ratios for the inward and outward migration. The final values of the semi-major axes and the eccentricities depend directly on the migration rates (or on the corresponding e -folding times) \dot{a}_1/a_1 , \dot{a}_2/a_2 and the eccentricity damping rates \dot{e}_1/e_1 , \dot{e}_2/e_2 (where indices '1' and '2' stay for the inner and outer planet, respectively), and not only on their ratios K_1 and K_2 . The characterisation of the system's final state by using the migration parameters will be discussed more detailed at the end of this section.

In the following we repeat the three-body calculations for GJ 876 by Lee & Peale (2002a) adding the effects of an inner disc, then we review the simulations for HD 73 526 by Sándor et al. (2007), and finally present our new results in modelling the formation of HD 82 943 and HD 128 311 with an inner disc.

4.1. GJ 876 and HD 73526

GJ 876: First we repeated the simulations of Lee & Peale (2002a) on the formation of GJ 876 by using three-body calculations with dissipative forces. Similarly to their results, we required $K_2 = \tau_{a_2}/\tau_{e_2} = 100$ if only the outer giant was affected by an outer disc. The evolution of the semi-major axes and the eccentricities is shown in the top panel of Fig. 12. In our calculations we used $\tau_{a_2} = 2 \times 10^4$ and $\tau_{e_2} = 2 \times 10^2$ years giving exactly $K_2 = 100$. We note again that this ratio between the e -folding times is very high and maybe physically unrealistic for massive planets.

To quantify the damping effect of the inner disc on the inner planet while the giant planets revolve in a common gap, we performed further three-body simulations with also $\tau_{a_1} = -2 \times 10^4$ and $\tau_{e_1} = 2.5 \times 10^3$ years, where we point out that the minus sign of τ_{a_1} stands for the outward migration. To model the damping effect of the outer disc on the outer planet we used the e -folding times $\tau_{a_2} = 2 \times 10^4$ and $\tau_{e_2} = 2.5 \times 10^3$ years. Note that the above migration parameters correspond to $K_1 = K_2 = 8$. The result of our calculations is shown in the bottom of Fig. 12. These figures in fact are very similar to those obtained by Lee & Peale (2002a), however to model the behaviour of the system, we used different migration parameters.

HD 73 526: As we already mentioned, the effect of an inner disc was studied more detailed by Sándor et al. (2007) in the

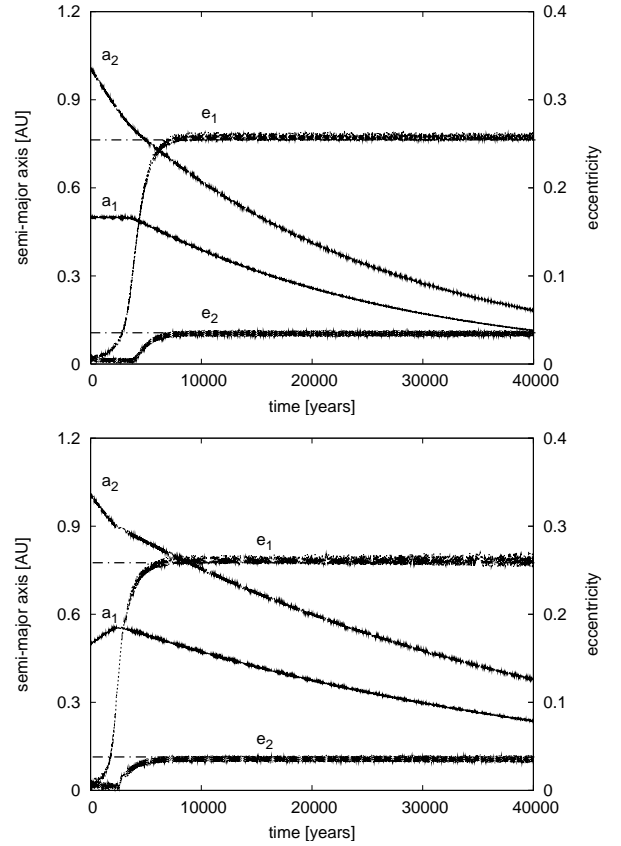


Fig. 12. Behaviour of the semi-major axes and the eccentricities of the resonant giant planets in the system GJ 876. The horizontal lines correspond to the observed values of the eccentricities. *Top:* Only the outer disc is taken into account, and therefore only the orbital evolution of the outer planet is affected, with the e -folding times $\tau_{a_2} = 2 \times 10^4$ years, $\tau_{e_2} = 2 \times 10^2$ years, so $K_2 = 100$. *Bottom:* Same as above in the presence of outer and inner discs. In this case, $\tau_{a_1} = -2 \times 10^4$, $\tau_{e_1} = 2.5 \times 10^3$, $\tau_{a_2} = 2 \times 10^4$, and $\tau_{e_2} = 2.5 \times 10^3$ years (giving $K_1 = K_2 = 8$).

case of HD 73 526. There, it has been shown that if the outer planet is damped only, one needs $K_2 = 15 - 20$, which according to the hydro-dynamical simulations seems to be a too high value. Moreover, if only the outer planet is damped, the eccentricity of the inner planet shows an increasing tendency, which can result in exceeding the limit coming from the observations ($e_{\text{inn}} \approx 0.3$). On the other hand, if in addition the inner planet is damped by an inner disc, the eccentricities will level off and the outcome of the migration scenario fits better to the observations: the formation of HD 73 526 could be modelled successfully by using the e -folding times $\tau_{a_1} = -5 \times 10^4$, $\tau_{a_2} = 10^4$ years and $\tau_{e_1} = 5 \times 10^3$, $\tau_{e_2} = 10^3$ (corresponding to $K_1 = K_2 = 10$). The behaviour of the eccentricities in this case is shown in the top panel of Fig. 8 in the paper of Sándor et al. (2007).

We can conclude that the presence and effect of an inner disc in modelling the formation processes of GJ 876 and HD 73 526 is physically more realistic, giving results fitting very well to the radial velocity observations. In what follows, we show that in the case of the systems HD 82 943 and HD 128 311 the presence of an inner disc is still a real alternative, however these systems do not need such strong dampings for the eccentricity of their inner giant planets.

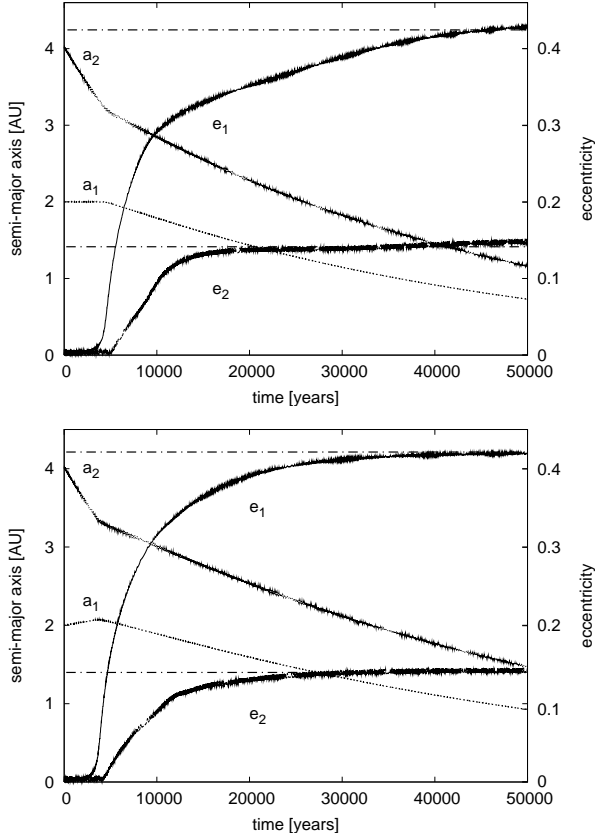


Fig. 13. Behaviour of the semi-major axes and the eccentricities of the giant planets in the resonant system HD 82943. The horizontal lines correspond to the observed values of the eccentricities. *Top*: Only the motion of the outer planet is affected, with the e -folding times $\tau_{a_2} = 2 \times 10^4$ and $\tau_{e_2} = 2.5 \times 10^3$ years ($K_2 = 8$). *Bottom*: An inner disc is also assumed, with $\tau_{a_1} = -2 \times 10^5$, $\tau_{e_1} = 5 \times 10^4$ years e -folding times for the inner planet ($K_1 = 4$), which allows the use of larger $\tau_{e_2} = 2.5 \times 10^3$ years and thus lower ratio $K_2 = 4$ for the outer planet.

4.2. HD 82943 and HD 128311

HD 82943: Recently Lee et al. (2006) presented four sets of orbital solutions based on a best-fit double-Keplerian model for HD 82943. Using their orbital elements as initial conditions, direct numerical integrations show that three of them exhibit ordered behaviour, while one (Fit I in the cited paper) is destabilised after a few thousand years. In one of the three dynamically stable orbital solutions (Fit II) the variations of the eccentricities are negligible, and the resonance variables oscillate with small amplitudes indicating clearly that the system is deep in the 2:1 MMR. Since this behaviour can be reached during an inward convergent migration of the giant planets, we investigate the formation of this system using the scenario of the planetary migration.

First we assume that only an outer disc is present and the outer planet feels its damping effect. To obtain the dynamical state calculated based on Fit II ($e_1 = 0.422$, $e_2 = 0.14$, $a_1 = 0.74$ AU, $a_2 = 1.18$ AU), we needed the ratio $K_2 = 8$, using $\tau_{a_2} = 2 \times 10^4$ and $\tau_{e_2} = 2.5 \times 10^3$ years. This ratio K_2 does not seem too high (as it lies typically between 1 and 10), however, similarly to HD 73526, the eccentricities are slightly increasing during the whole migration process. This is not a problem if the migration of the planets is terminated gradually around

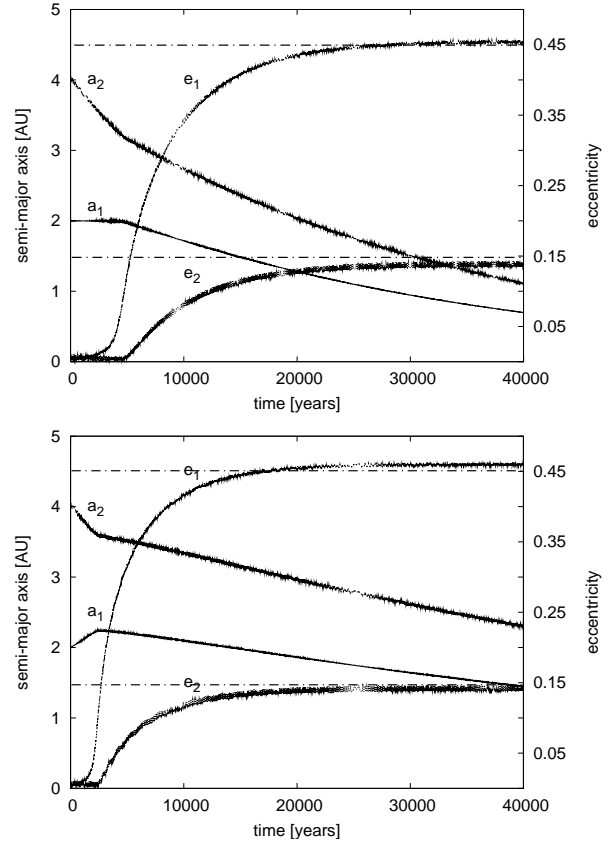


Fig. 14. Behaviour of the semi-major axes and the eccentricities of the resonant giant planets in the resonant system HD 128311. The horizontal lines correspond to the observed values of the eccentricities. *Top*: Only the motion of the outer planet is damped by an outer disc, with $K_2 = \tau_{a_2}/\tau_{e_2} = 7$. *Bottom*: An inner disc is also assumed. The e -folding times for the inner planet are $\tau_{a_1} = 2 \times 10^4$, $\tau_{e_1} = 10^4$ years ($K_1 = 2$), which allows to use much lower ratio $K_2 = 2$ for the outer planet.

the observed values of their semi-major axes but it may result in exceeding the limits derived from observations, see the top panel of Fig. 13. On the other hand, by assuming the presence of an inner disc, the eccentricities reach their constant values gradually which do not seem to change further during the migration process. The latter behaviour is shown in the bottom panel of Fig. 13. During this simulation we used for the inner planet $\tau_{a_1} = -2 \times 10^5$ and $\tau_{e_1} = 5 \times 10^4$ years, and for the outer planet $\tau_{a_2} = 2 \times 10^4$ and $\tau_{e_2} = 5 \times 10^3$ years (giving $K_1 = K_2 = 4$). Since the eccentricities seem to reach constant values, this case seems to be a more convenient formation scenario for HD 82943 than the previous one.

We can conclude that the present dynamical behaviour of the resonant system HD 82943 (based on Fit II of Lee et al. (2006)) can be explained in both ways: by assuming an outer disc alone or by assuming an inner and an outer disc. However, the latter case seems to be more reasonable since when the migration occurs over longer times it guarantees constant eccentricity values during the whole process.

HD 128311: Finally, we present our results for HD 128311. The most recent orbital solution for this system is presented by Vogt et al. (2005), while possible formation scenarios are outlined by Sándor & Kley (2006). In the latter study, the formation

of the resonant system is modelled by an inward convergent migration of the giant planets which is followed by a sudden perturbation; only the effect of an outer disc was considered. Prior to the sudden perturbation, the outer giant planet migrated inward and captured the inner one into a 2:1 resonance. It is essential to find the final values of the eccentricities as due to the migration process since the perturbative events modify only their oscillations. These values are $e_1 \approx 0.45$ and $e_2 \approx 0.15$ being obtained after a migration characterised by $K_2 = \tau_{a_2}/\tau_{e_2} = 5$. In the present study we need somewhat larger ratio, $K_2 = 7$, since contrary to Sándor & Kley (2006), we do not stop the migration when the planets reach their actual positions. The evolution of the semi-major axes and eccentricities are presented in the top panel of Fig. 14.

Assuming an inner disc, the same final state of the migratory evolution of HD 128 311 can be obtained. In our numerical experiments we used $\tau_{a_1} = -2 \times 10^4$, $\tau_{e_1} = 10^4$ years for the inner planet, and $\tau_{a_2} = 2 \times 10^4$, $\tau_{e_2} = 10^4$ years for the outer planet (being equivalent to $K_1 = K_2 = 2$). The evolution of the system is shown in the bottom panel of Fig. 14. Comparing the top and the bottom panels of Fig. 14, we can conclude that the formation of HD 128 311 can also be modelled by assuming an inner disc, however in this particular case, this is not definitely necessary.

4.3. Final state of a migration with an inner disc: Numerical experiments

In this part we show the results of additional numerical simulations in which we studied how the different parameters of migration influence the final state of the resonant system. It was quite evident from the beginning that the characterisation based only on the ratios K_1 and K_2 would not yield unique results in the case when the inner planet is also affected by an inner disc.

Our calculations are based on the observed orbital and physical parameters of GJ 876, as given by Lee & Peale (2002a). For the inward migration of the outer planet we fixed $\tau_{a_2} = 4 \times 10^4$, $\tau_{e_2} = 5 \times 10^3$ years (so, $K_2 = 8$), and we changed τ_{a_1} and τ_{e_1} in such a way to obtain the observed state of the system.

As starting values to our numerical simulations we used $\tau_{a_1} = -3 \times 10^4$ years and found that $\tau_{e_1} = 3.7 \times 10^3$ years gives a correct result ($K_1 \approx 8$ here). Then we increased gradually the absolute value of τ_{a_1} corresponding to a weaker damping on a_1 . To obtain the observed behaviour of the system, for larger τ_{a_1} , we needed larger τ_{e_1} meaning a weaker damping on e_1 too. In order to explore the mutual dependence of τ_{a_1} and τ_{e_1} , we performed a series of numerical experiments. Our results are shown in Fig. 15; on the x -axis the absolute value of τ_{a_1} , while on the y -axis the eccentricity damping time τ_{e_1} are displayed in logarithmic scale. The crosses show those corresponding values of τ_{a_1} and τ_{e_1} which are needed to obtain the same final values of the eccentricities e_1 and e_2 (0.26 and 0.035 respectively). The τ_{e_1} increases rapidly for small $|\tau_{a_1}|$, however it is not proportional to τ_{a_1} (compare with the straight line on Fig. 15), but it levels off and clearly tends to a limit $\tau_{e_1\max}$, which in this case is slightly higher than 9×10^3 years.

We can conclude that for a fixed pair of τ_{a_2} and τ_{e_2} , there is no unique K_1 that determines the final state of the system. On the contrary, there exists a $\tau_{e_1\max}$, which determines the final state of the system if the inner disc does not affect the semi-major axis of the inner planet. In reality, however, the inner disc (as rotating faster) can transmit angular momentum to the inner planet as well as energy, increasing its semi-major axis. In this case we need smaller τ_{e_1} , or equivalently, more effective damping on e_1 .

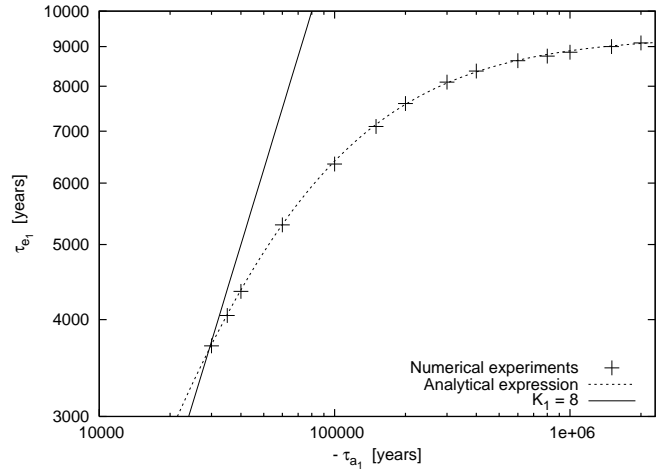


Fig. 15. Pairs of migration parameters τ_{a_1} and τ_{e_1} which result in the observed state of the system GJ 876 for fixed $\tau_{a_2} = 4 \times 10^4$ years and $\tau_{e_2} = 5 \times 10^3$ years. *Crosses*: Empirically found with N-body simulations. *Dashed curve*: Analytical expression Eq. (16) (see Sect. 4.4). *Solid line*: Constant ratio $K_1 = 8$, for comparison.

If we compare the two migration scenarios: (i) only an outer disc is present and there is no inner disc between the inner planet and the star; and (ii) both an outer disc and an inner disc are present and the planets orbit in a common gap between them, we can summarise the following results: The final state of the system in case (i) can be described solely by the ratio $K_2 = \tau_{a_2}/\tau_{e_2}$. In case (ii), the ratios K_1 and K_2 are not enough, the final state of the system depends on additional parameters too; in the most general case, when the inner disc forces the inner planet to migrate outward, there are essentially three parameters, which can be K_1 , K_2 , and the ratio τ_{a_1}/τ_{a_2} for instance. In next subsection, we analyse theoretically this behaviour.

4.4. Final state of a migration with an inner disc: Analytics

For the semi major axis and eccentricity of a planet to decrease exponentially with damping timescales $\tau_a = -\dot{a}/a$ and $\tau_e = -\dot{e}/e$, its energy E and angular momentum H must vary with the following rates (through Eqs. (2) and (3)):

$$\dot{E} = E/\tau_a \quad (6)$$

$$\dot{H} = \frac{H}{2} \left(\frac{2e^2}{1-e^2} \frac{1}{\tau_e} - \frac{1}{\tau_a} \right) \quad (7)$$

When two planets are considered, the variation of the energy of the system { pair of planets }, \dot{E} is the sum of the energy variations applied to both planets, so that

$$\dot{E} = \frac{E_1}{\tau_{a_1}} + \frac{E_2}{\tau_{a_2}}. \quad (8)$$

If the two planets are in resonance, the ratio between their semi major axes is kept constant, and consequently also the ratio between their energies. Let us define:

$$\varepsilon = E_2/E_1 = M_2 a_1 / M_1 a_2. \quad (9)$$

Then,

$$E = E_1 + E_2 = (1 + \varepsilon)E_1, \quad (10)$$

$$\dot{E} = (1 + \varepsilon)\dot{E}_1. \quad (11)$$

Note that due to some energy exchange between the planets through the resonance, the variation of the energy of the first planet is not E_1/τ_{a_1} , but $\dot{E}_1 = \dot{E}/(1+\varepsilon)$, with \dot{E} given by Eq. (8).

The same holds for the angular momentum. For the angular momentum H of the system { pair of planets } ($H = H_1 + H_2$), the total variation rate reads (from Eq. (7)) :

$$\dot{H} = \sum_{i=1,2} \frac{H_i}{2} \left(\frac{2e_i^2}{1-e_i^2} \frac{1}{\tau_{e_i}} - \frac{1}{\tau_{a_i}} \right). \quad (12)$$

For the final state, when the planets are in resonance and their eccentricities are also constant, as is the ratio of their angular momentum. Let us define :

$$\eta = H_2/H_1 = \frac{M_2}{M_1} \sqrt{\frac{a_2(1-e_2^2)}{a_1(1-e_1^2)}}. \quad (13)$$

Then, $H = H_1 + H_2 = (1+\eta)H_1$, and also

$$\dot{H} = (1+\eta)\dot{H}_1. \quad (14)$$

If the eccentricities are constant ($\dot{e}_i = 0$), then, from Eqs. (3), (10), (11), and finally (8) :

$$\dot{H}_i = -\frac{H_i}{2} \frac{\dot{E}_i}{E_i} = -\frac{H_i}{2} \frac{\dot{E}}{E} = -\frac{H_i}{2} \left(\frac{1/\tau_{a_1} + \varepsilon/\tau_{a_2}}{1+\varepsilon} \right) \quad (15)$$

Using Eqs. (12) and (15), Eq. (14) gives a relation between τ_{a_1} , τ_{a_2} , τ_{e_1} , and τ_{e_2} . In the problem that we study, the masses of the planets are known, as well as their eccentricities and the ratio between their semi major axes. The question is : for a given effect on the outer planet, what should the effect on the inner planet be to be consistent with the observed eccentricities ? Below, we solve this equation in the unknown τ_{e_1} with the free parameter τ_{a_1} , while τ_{a_2} , τ_{e_2} , ε and η , are given constants (ε and η being defined by Eqs. (9) and (13) respectively). Using Eqs. (12) and (15), Eq. (14) reads :

$$\begin{aligned} \sum_{i=1,2} \frac{H_i}{2} \left(\frac{2e_i^2}{1-e_i^2} \frac{1}{\tau_{e_i}} - \frac{1}{\tau_{a_i}} \right) &= -(1+\eta) \frac{H_1}{2} \left(\frac{1/\tau_{a_1} + \varepsilon/\tau_{a_2}}{1+\varepsilon} \right) \\ \frac{2e_1^2}{1-e_1^2} \frac{1}{\tau_{e_1}} - \frac{1}{\tau_{a_1}} + \eta \left(\frac{2e_2^2}{1-e_2^2} \frac{1}{\tau_{e_2}} - \frac{1}{\tau_{a_2}} \right) &= -\frac{1+\eta}{1+\varepsilon} \left(\frac{\varepsilon}{\tau_{a_2}} + \frac{1}{\tau_{a_1}} \right) \\ \frac{2e_1^2}{1-e_1^2} \frac{1}{\tau_{e_1}} &= \frac{1}{\tau_{a_2}} \left(\eta - \frac{(1+\eta)\varepsilon}{1+\varepsilon} \right) - \frac{1}{\tau_{e_2}} \frac{2e_2^2\eta}{1-e_2^2} + \frac{1}{\tau_{a_1}} \left(1 - \frac{1+\eta}{1+\varepsilon} \right). \end{aligned}$$

Eventually, we obtain :

$$\frac{1}{\tau_{e_1}} = \underbrace{\frac{1-e_1^2}{2e_1^2} \left(\frac{1}{\tau_{a_2}} \frac{\eta-\varepsilon}{1+\varepsilon} - \frac{1}{\tau_{e_2}} \frac{2e_2^2\eta}{1-e_2^2} \right)}_{1/\tau_{e_1\max}} + \underbrace{\frac{1}{\tau_{a_1}} \frac{1-e_1^2}{2e_1^2} \frac{\varepsilon-\eta}{1+\varepsilon}}_{K_{1,0}} \quad (16)$$

As one can see, the damping rate that should be applied to the inner planet ($1/\tau_{e_1}$) is the sum of two terms.

The first one ($1/\tau_{e_1\max}$) is required to balance the action on the outer planet ; indeed, when no force is applied to the inner planet, the energy loss rate of the outer planet is not the expected E_2/τ_{a_2} , but $(E_2/\tau_{a_2}) \frac{\varepsilon}{1+\varepsilon}$ because the inner planet also has to lose energy to preserve the resonant motion ; thus, the angular momentum loss rate is overestimated by the expression Eq. (7), and both eccentricities rise. Therefore, a damping of the eccentricity needs to be applied on the inner planet as well.

The second term ($K_{1,0}/\tau_{a_1}$) is proportional to $\tau_{a_1}^{-1}$; the coefficient $K_{1,0}$ is negative if $e_1^2 > (1 - (a_2/a_1)^3) + (a_2/a_1)^3 e_2^2$, which is always true in the case of a 2:1 MMR for $e_2 < 0.866$.

In the case studied in the previous Sect. 4.3, one has (Lee & Peale 2002a) : $M_2 = 1.808 M_{\text{Jup}} = 5.65 \times 10^{-3} M_*$, $M_1 = 0.5696 M_{\text{Jup}} = 1.78 \times 10^{-3} M_*$, $e_1 \approx 0.265$, $e_2 \approx 0.035$, $\tau_{a_2} = 4 \times 10^4$, $\tau_{e_2} = 5 \times 10^3$ and the two planets are in 2:1 MMR, with $a_2/a_1 = 1.602$. Thus, $\eta = 4.1641$ and $\varepsilon = 1.9812$. This gives $\tau_{e_1\max} = 9289$ years, and $K_{1,0} = -4.8471$. The dashed curve on Fig. 15 shows τ_{e_1} as a function of τ_{a_1} from Eq. (16). The fit is excellent.

This shows that Eq. (16) efficiently gives what parameters one should choose to reproduce a given system by the means of N-body simulations with dissipative forces, or one should have in the protoplanetary disc. In particular, the expression of $\tau_{e_1\max}$ shows that if e_2 is relatively small, a huge K_2 of the order of e_2^{-2} is required for $\tau_{e_1\max} \rightarrow \infty$. If the inner disc tends to make the inner planet migrate outward with $\tau_{a_1} < 0$, an additional damping on its eccentricity is required, which can be expressed as $\tau_{e_1\text{add}} = \tau_{a_1}/K_{1,0}$, with $K_{1,0} < 0$, depending on all the parameters of the system. On the other hand, if the inner disc tends to attract the planet sufficiently (which may happen as has been shown in Sect. 2), no eccentricity damping on the inner planet may be required at all (this happens in our case if $\tau_{a_1} = +45025$ years).

With this equation, one can try to find reasonable parameters (with not too big K_1 and K_2) to explain how all the known resonant exoplanetary systems can have been formed in the disc. Our numerical simulations have shown that this can be achieved for at least 4 such systems.

5. Conclusion

In this paper, we address the problem of the moderate eccentricity of extra-solar planets in resonance. The resonant configuration requires a convergent migration of the planets, but continued migration in resonance leads to unlimited eccentricity growth if no eccentricity damping mechanism is at work.

In Sect. 2, we have shown that an inner disc has a non negligible influence on a giant planet on an eccentric orbit and modifies its orbital parameter. The strength of this effect varies with planetary eccentricity. For very small eccentricities, $e \leq 0.05$, we find a very small but positive \dot{e} while for larger e it becomes more and more negative. The induced change in semi-major axis remains positive, as expected for the Lindblad torques induced by an inner disc on a massive planet. Only for larger eccentricities $e \geq 0.35$ the change in semi-major axis becomes negative, leading to inward migration. The usage of a constant K -factor between the e -folding time scales of the semi-major axis and the eccentricity is clearly an over simplification.

However, the measured influence of the disc on the planet depends on the adopted tapering function applied to exclude at least parts of the gas within the Hill sphere of the planet, and possibly on other numerical effects, such as the smoothing length, the resolution, or boundary conditions. Hence, determination of the exact, absolute magnitude of the effect is a bit difficult.

Anyway, an eccentricity damping should be applied to the inner planet to obtain realistic results, in particular if its eccentricity is larger than 0.1. Using a hybrid 2D-1D hydro-code that allows the simulation of the whole disc from its physical inner boundary to an arbitrary large radius, we compute the longterm evolution of the GJ 876 system, for which the orbital elements are well known, and the radius of the inner edge of the disc can be estimated thanks to the presence of a third planet very close

to the star. We find that the inner disc does not disappear after the planets opened a common gap, and that it effectively helps damping the eccentricity of the inner planet. With realistic disc parameters (viscosity and aspect ratio), we are able to reproduce the observations.

As hydro-simulations are very time-consuming, we finally perform customised N-body simulations with explicit non-conservative forces, added to mimic the effect of the outer and inner disc. We find that applying a significant damping to both planets, as required by the influence of both the inner and outer discs, enables us to fit quite well a few other exoplanetary systems. In addition, N-body simulations have shown that when two planets are considered, the ratio between the eccentricity and semi major axis damping applied on each of them (K_1 and K_2) are not sufficient to determine the final state of the system. In fact, for a given damping in a and e applied on the outer planet, one can express analytically the eccentricity damping that should be applied on the inner planet to match the observed orbital configuration, as a function of its semi major axis damping.

Given the satisfying fits of a few systems that we obtain, we claim that the problem of the low eccentricities of the resonant exoplanetary systems simply stems from the fact that the inner disc had not been taken properly into account, which is not reasonable. A pair of planets orbiting in a protoplanetary disc may well orbit in a common gap and enter a Mean Motion Resonance, but it does not necessarily open a complete cavity from the star to the outermost planet, so that the inner disc should influence the planets dynamics. Crida & Morbidelli (2007) already suggested that the opening of such a cavity by a giant planet requires very specific conditions; in fact, according to our hydro and N-body simulations, the low observed eccentricities of the exoplanets in resonance support the idea that the inner disc does not disappear in general.

Acknowledgements. A. Crida acknowledges the support through the German Research Foundation (DFG) grant KL 650/7. Zs. Sándor thanks the supports of the Hungarian Scientific Research Fund (OTKA) under the grant PD48424 and of the DFG under the grant 436 UNG 17/1/07.

Very fruitful discussions with F. Masset and C. Dullemond are gratefully acknowledged.

References

- Beaugé, C., Michtchenko, T. A., & Ferraz-Mello, S. 2006, MNRAS, 365, 1160
 Bryden, G., Różyczka, M., Lin, D. N. C., & Bodenheimer, P. 2000, ApJ, 540, 1091
 Cresswell, P., Dirksen, G., Kley, W., & Nelson, R. P. 2007, A&A, 473, 329
 Crida, A. & Morbidelli, A. 2007, MNRAS, 377, 1324
 Crida, A., Morbidelli, A., & Masset, F. 2006, Icarus, 181, 587
 —. 2007, A&A, 461, 1173
 D’Angelo, G., Lubow, S. H., & Bate, M. R. 2006, ApJ, 652, 1698
 Goldreich, P. & Tremaine, S. 1979, ApJ, 233, 857
 —. 1980, ApJ, 241, 425
 Kley, W. 2000, MNRAS, 313, L47
 Kley, W. & Dirksen, G. 2006, A&A, 447, 369
 Kley, W., Lee, M. H., Murray, N., & Peale, S. J. 2005, A&A, 437, 727
 Kley, W., Peitz, J., & Bryden, G. 2004, A&A, 414, 735
 Kley, W. & Sándor, Z. 2007, in Extrasolar Planets: Formation, Detection and Dynamics, ed. R. Dvorak, 945–
 Laughlin, G., Butler, R. P., Fischer, D. A., et al. 2005, ApJ, 622, 1182
 Lee, M. H., Butler, R. P., Fischer, D. A., Marcy, G. W., & Vogt, S. S. 2006, ApJ, 641, 1178
 Lee, M. H. & Peale, S. J. 2002a, ApJ, 567, 596
 —. 2002b, ApJ, 567, 596
 Lin, D. N. C. & Papaloizou, J. 1979, MNRAS, 186, 799
 Lubow, S. H. 1991, ApJ, 381, 259
 Masset, F. 2000a, A&AS, 141, 165
 Masset, F. 2000b, in ASP Conf. Ser. 219: Disks, Planetesimals, and Planets, ed. G. Garzón, C. Eiroa, D. de Winter, & T. J. Mahoney, 75–80
 Masset, F. & Snellgrove, M. 2001, MNRAS, 320, L55
 Masset, F. S., Morbidelli, A., Crida, A., & Ferreira, J. 2006, ApJ, 642, 478
 Morbidelli, A. & Crida, A. 2007, Icarus, 191, 158
 Morbidelli, A., Tsiganis, K., Crida, A., Levison, H. F., & Gomes, R. 2007, ArXiv e-prints, 706
 Papaloizou, J. C. B. 2003, Celestial Mechanics and Dynamical Astronomy, 87, 53
 Papaloizou, J. C. B., Nelson, R. P., & Masset, F. 2001, A&A, 366, 263
 Sándor, Z. & Kley, W. 2006, A&A, 451, L31
 Sándor, Z., Kley, W., & Klagyivik, P. 2007, A&A, 472, 981
 Shakura, N. I. & Sunyaev, R. A. 1973, A&A, 24, 337
 Snellgrove, M. D., Papaloizou, J. C. B., & Nelson, R. P. 2001, A&A, 374, 1092
 Tanaka, H. & Ward, W. R. 2004, ApJ, 602, 388
 Thommes, E. W., Bryden, G., Wu, Y., & Rasio, F. A. 2007, ArXiv e-prints, 706
 Vogt, S. S., Butler, R. P., Marcy, G. W., et al. 2005, ApJ, 632, 638